Simulation of a High Voltage System in a Hybrid Electrical Vehicle

Rüdiger Appunn and Kay Hameyer
Institute of Electrical Machines, RWTH Aachen University
ruediger.appunn@iem.rwth-aachen.de, kay.hameyer@iem.rwth-aachen.de

***Abstract*-In modern hybrid electrical vehicles (HEV) the electrical system includes different voltage levels. Visualization of the electric quantities such as currents and voltages of a high voltage system under load conditions is presented in this paper. Different strategies of electric component modeling such as machines or power electronics are used for an intensive analysis of the electrical system. Evaluation of the DC-link with respect to transients and feedbacks resulting from operational performance or fault operation is done.**

***Keywords*-hybrid electrical vehicle (HEV), vehicle electrical system, high voltage system, electric component modeling, voltage transients, DC-link**

I. Introduction

Nowadays an increasing number of (hybrid) electrical vehicles are fabricated. New challenges regarding reliability and safety arise as high voltage systems are used in new generations of vehicles. Observing currents and voltages in electrical systems of HEV during operation is essential for the performance and stable operation of the vehicle. Detailed system simulation is presented here to examine these parameters. This paper focuses on the visualization of dynamic behavior of voltages and currents resulting from the operation of the vehicle. Hereby influences on single system components can be evaluated and a life cycle analysis is supported. Components of the electrical system can be described by their transfer functions. This signal flow oriented method of simulation can be found in literature [1]. Another approach to model the system components is the use of electric equivalent circuits [2]. A combination of both methods, which exploits the advantages of both, is presented in this work.

II. Information

A. Topology of the vehicle electrical system

The investigated high voltage system of the vehicle and the connection to the low-volt system are shown in Figure 1. There are three voltage levels, variable high voltage AC, fixed high voltage DC and low voltage DC (12V system). The HV-system is built with two separated cables for HV+ and HV-, which are insulated from the car chassis at 12V- potential. Y-capacitors between HV potential and chassis are installed for EMC. The starter/generator, a permanent magnet excited synchronous machine (PMSM), either operates in generator mode or supports the internal combustion engine during motor boost operation. It serves as a starter-motor and allows energy recuperation at braking operation. Start-Stop operation in inner city areas is possible, too. The power electronics (PE), a converter/ rectifier topology consisting of six switches enables bidirectional energy flow. The semiconductors, here IGBTs are controlled by different control loops for each operation. The distribution unit (DU) connects HV-battery system, starter/generator, HV load and the DC-DC converter. The HV-battery system, a lithium-ion battery provides a voltage above 100V. The HV load is a consumer positioned in HV-system. Electric air conditioners or other auxiliary drives can be placed here. A DC-DC converter connects the HV-system with the 12V level. Bidirectional energy flow is possible. The LV-system and all consumers and components are summarized in one function block.

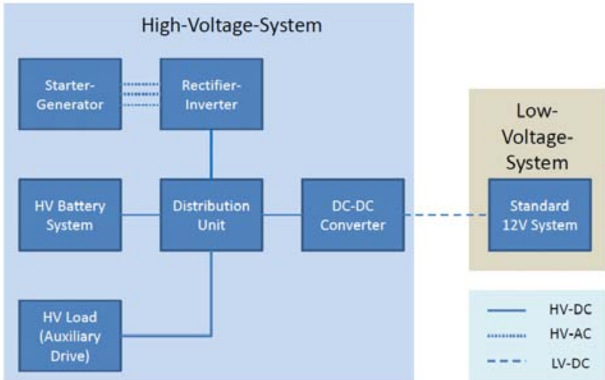

Fig. 1. Topology of the vehicle electrical system.

B. Component modeling

The components of the vehicle electrical system are modeled by their transfer functions and equivalent electric circuits with concentrated parameters. In this work the Piece-wise Linear Electrical Circuit Simulation (PLECS) [3] software is used to model the PE circuit. Hereby electric circuits can be integrated into a Matlab/Simulink model and an interaction between the two modeling strategies is possible.

The PLECS-model used is shown in Figure 2. It corresponds to the general topology of the studied high voltage system. There are some additional elements which are used to model the electric phenomena, like voltage transients, during operation. A detailed description of the different component modeling strategies is presented.

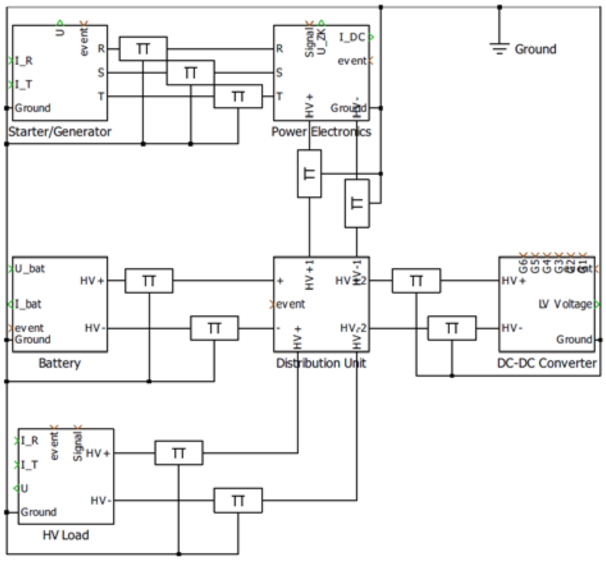

Fig. 2. HV-system modeled in PLECS

For the Starter/Generator a PMSM-model in dq-axis is applied. The differential equations, of this system are

$$T_d \cdot \frac{di_d}{dt} + i_d = \frac{u_d}{R_1} + \omega \cdot T_q \cdot i_q \quad (1)$$

$$T_q \cdot \frac{di_q}{dt} + i_q = \frac{u_q}{R_1} - \omega \cdot T_d \cdot i_d - \frac{\omega \cdot L_{hd}}{R_1} \cdot i'_{F0} \quad (2)$$

$$\frac{J}{p} \cdot \frac{d\omega}{dt} = p \cdot \left[i'_{F0} \cdot L_{hd} - i_d \cdot \left(L_q - L_d \right) \right] \cdot i_q - M_W \quad (3)$$

where $T_d = \frac{L_d}{R_1}$ and $T_q = \frac{L_q}{R_1}$.

These machine equations are implemented in a block diagram in the Simulink environment (Figure 3) and interact with the circuit simulator by controlling the current sources of the machine model. Figure 4 shows the current sources Ia and Ic, which impress the stator currents from the machine model to the clamps of its representation in the electric circuit environment. The phase to phase voltages are measured here as well and serve as inputs for the machine equations in the Simulink environment.

For accurate simulation of the generator mode in dynamic operation, the internal combustion engine (ICE) is modeled, too. By using the Matlab toolbox SimDriveline, it is possible to model the mechanical drive train components and couple them with the electrical machine model. The ICE is simulated by a lookup table which determines the torque applied to the shaft depending on torque demands regarding the actual speed of the motor. It is possible to define additional torques and moments of inertia. In this way the complete, hybrid drive train can be modeled. Figure 5 presents the mechanical drive train modeled in Simulink.

The power electronics is simulated by switching devices and freewheeling diodes (Figure 6). In this simulation IGBTs are used. Control loops at the Simulink environment control the semiconductor switches via Space Vector Modulation [4,5].

The dynamic battery model is based on a modified Thevenin model [6]. Figure 7 shows the electric equivalent circuit. It consists of the open-circuit voltage source U_0, the inner resistance R_i, a parallel RC-element simulating transient behavior and the series inductance L_i of the contacts. The Voltage U_0 is depending on the state of charge (SOC) of the battery. Equation 4 defines the SOC of the battery:

$$SOC = \frac{C - Q_{Dis}}{C} \quad (4)$$

Where C is the Capacity and Q_{Dis} the discharged electrical charge of the battery. The voltage of one Li-Ion cell in function of the SOC is presented in Figure 8 [7]. The battery consists of 33 cells. Transient charging/ discharging phenomena can be simulated.

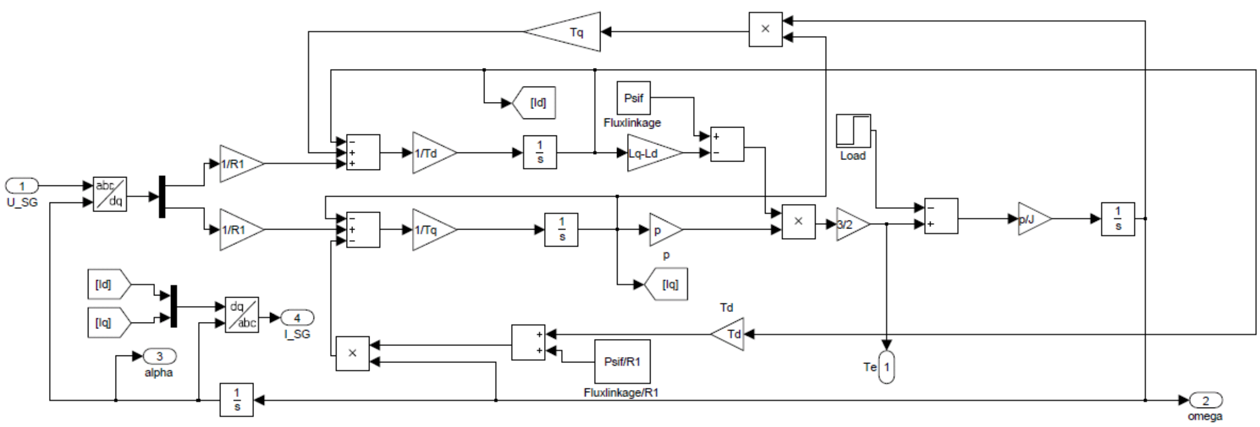

Fig. 3. Dynamic machine model of a PMSM in Simulink.

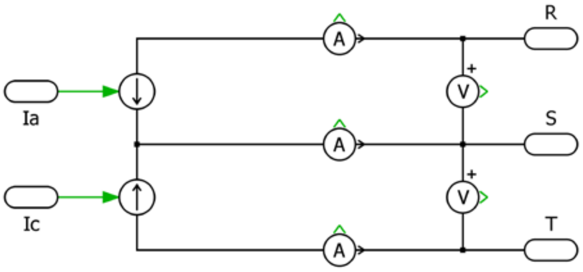

Fig. 4. Voltage controlled current sources representing the PMSM in the circuit simulator.

The load in the HV-system is an auxiliary drive, for instance an electrical climate control unit. A PMSM machine model and a pulse-controlled inverter are implemented in this simulation. Similar modeling strategies for the electrical machine and the PE are utilized. Variable load cases can be simulated and studied.

The DC-DC converter consists of a high frequency switching unit including a transformer to separate the two voltage levels [8,9,10]. Figure 9 shows its topology. A filter capacitor on each side reduces voltage ripples in the DC-link. The 12V load is being characterized by a load resistor R_{load}. Since the focus of this vehicle electrical system simulation concentrates on the HV-system, this simplification is appropriate.

Power cables in the vehicle are simulated using π-equivalent circuits with line resistance, leakage inductance and capacitance to the car chassis (Figure 10). Herewith modeling of transients in the cable harness during dynamic operation is possible [11].

The peripheral line represents the vehicle body at LV-DC minus potential. Due to possible leakage currents to other electrical components of the vehicle, the car chassis is part of the model. Figure 11 shows the standardized structure of the interconnection from a HV-component to vehicle chassis. Y-capacitors and insulation resistances which can be reduced by switches are implemented.

Event ports can be used to simulate deviations from regular operation, such as load dumps. They are standardized and control the switches which reduce component parameters or change the electric circuit.

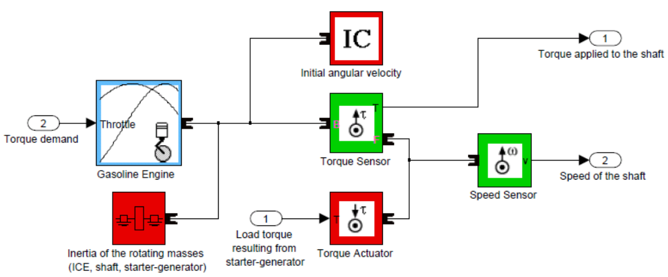

Fig. 5. Representation of the mechanical drive train modeled in Simulink.

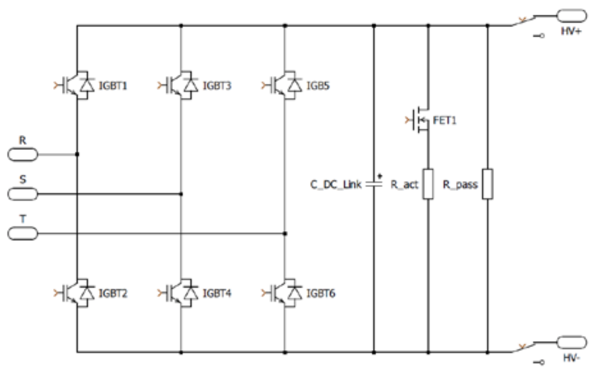

Fig. 6. Power electronics circuit in the HV-system.

C. Control

Control loops are implemented in the Simulink level. Torque and speed control for the starter/generator in motor operation or additional drives in the HV-System is realized by using field oriented control strategies. Figure 12 shows the implemented speed control. A cascade control of current and speed is used to adjust the speed. Hereby a dynamic load for the vehicle electrical system is simulated.

In generator operation the terminal voltage of the starter/generator (a PMSM) must be controlled by the power electronics, since no excitation current can be modified. Here an active rectifying method to control the charging current based on [12] and [13] is used.

Provided that symmetric three phase sinusoidal currents

$$\begin{bmatrix} i_R \\ i_S \\ i_T \end{bmatrix} = \hat{I} \cdot \begin{bmatrix} \cos \omega t \\ \cos(\omega t - \frac{2\pi}{3}) \\ \cos(\omega t + \frac{2\pi}{3}) \end{bmatrix} \quad (5)$$

exists in the stator windings, all harmonics are neglected and no saturation occurs, two phase currents have to be measured and transformed to an orthogonal system to calculate the current amplitude. The following transformation is used:

$$\begin{bmatrix} i_A \\ i_B \end{bmatrix} = T_{32} \begin{bmatrix} i_R \\ i_S \end{bmatrix}$$

$$T_{32} = \begin{bmatrix} \sqrt{\frac{3}{2}} & 0 \\ \frac{1}{\sqrt{2}} & \sqrt{2} \end{bmatrix} \quad (6)$$

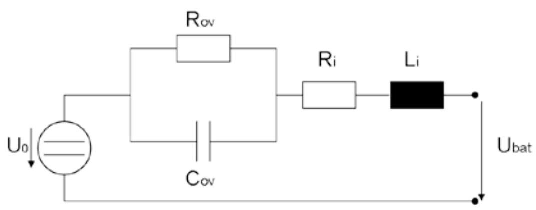

Fig. 7. Battery model based on Thevenin equivalent circuit[6].

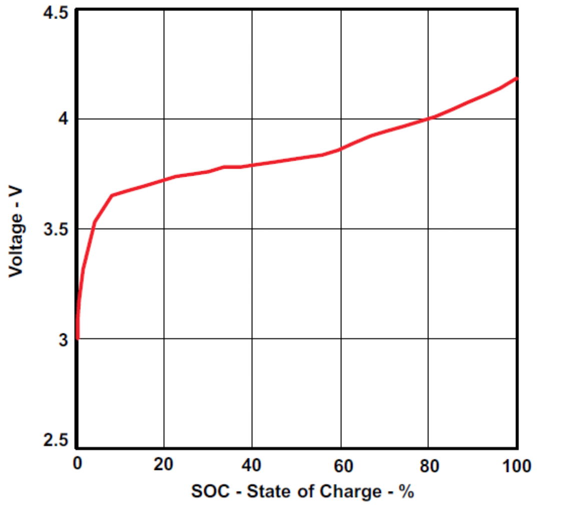

Fig. 8. No load voltage-state of charge characteristic of one Li-Ion cell [7].

From the orthogonal system the amplitude is determined via a dq-transformation:

$$\begin{bmatrix} i_d \\ i_q \end{bmatrix} = T_\alpha \begin{bmatrix} i_A \\ i_B \end{bmatrix}$$
$$T_\alpha = \begin{bmatrix} \cos(\alpha) & \sin(\alpha) \\ -\sin(\alpha) & \cos(\alpha) \end{bmatrix} \tag{7}$$

Where $\alpha = \omega t = \arctan \frac{i_B}{i_A}$.

The result is that $i_d = \hat{I}$, the current amplitude and $i_q = 0$.

The actual voltage control is applied by a cascade control. An outer voltage loop compares the DC-link with the desired voltage and serves as input for a PI-controller. Its output is added to the DC current, compared with the calculated current amplitude $\hat{I}$ and given to a PI-controller as well, this is the inner current control loop. By using the inverse transformations T_α^{-1} and T_{32}^{-1} the control output can be transformed to three phase values and the semiconductor switches are controlled via pulse width modulation. Figure 13 shows the control topology.

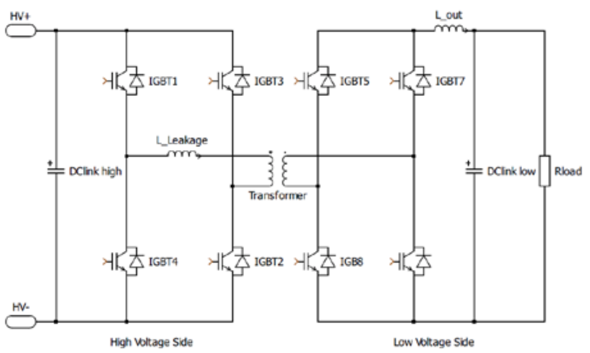

Fig. 9. Bidirectional DC-DC converter.

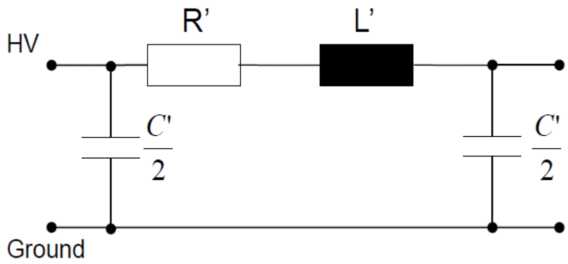

Fig. 10. π-equivalent circuit of HV-cable segment.

The bidirectional DC-DC converter has a closed loop control for energy flow from HV-system to the 12V system. It works as a step-down converter with additional PID controller. This is the nominal operation mode, since the starter/generator powers the low voltage system. For reverse energy flow the converter operates in step-up mode. An open loop controlled is implemented. This control method is sufficient, since only in fault cases the LV-system has to supply the HV-system. Figure 14 depicts the main control circuit.

D. Simulation

Depending on the particular drive cycle of the HEV several operation modes of the starter/generator are studied. Generator mode at varying speed and boost cycles with torque demands are considered. Start-stop mode and recuperative breaking are implemented in the model. Different operating conditions and their effects on the HV-DC link are simulated as well. Turn on, turn off (under load), dynamic load fluctuation, voltage and current ripples caused from HV components and state of charge HV-battery system variations are considered. Deviations from such operation conditions are studied. Here, transients resulting from a load dump or deterioration effects can be simulated by ideal switches or parameter variation. Coupling effects between the voltage levels are simulated as well. By these simulations a detailed evaluation of the HV-DC link with respect to voltage oscillations and internal feedbacks is possible. Four simulation results of fault situations are presented in the following paragraphs. The parameters of a topical hybrid electrical vehicle with a nominal DC-link voltage of above 100V are used.

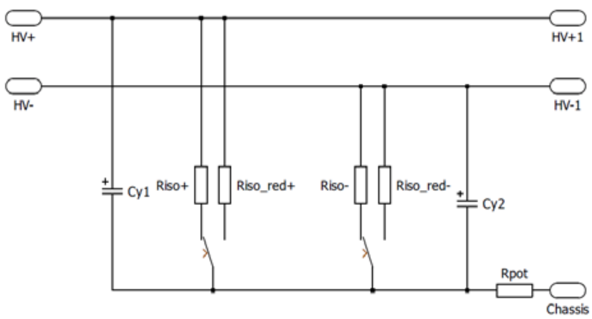

Fig. 11. Modeling of the chassis.

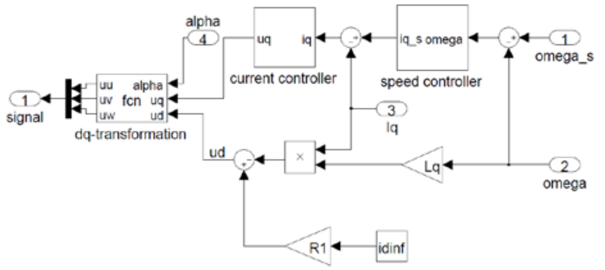

Fig. 12. Speed control of the PMSM.

1) Single insulation fault in the HV-system

Due to the fact, that the HV-system is built with two separated cables electrically insulated from the car chassis, a single insulation error does not cause a breakdown of the DC-link circuit. In Figure 15 the fault case occurs at 0.15 seconds. The former symmetric potentials of HV+ and HV- displace in positive direction. It can be seen that the DC-link voltage remains constant. So a single insulation fault is not critical for stable operation of the HV-system (insulated grid). The problem is that now HV- potential is connected to the car chassis and to 12V- potential. For safety issues the single insulation fault is critical and has to be detected.

2) Short circuit fault in DC-link circuit

Switching errors in power electronics or wrong maintenance can lead to short circuit faults in the HV-system. In Figure 16 the DC-link is short circuited at 0.15 seconds. The voltage decreases immediately and a high short circuit current occurs. Due to π-element cable modeling, small oscillations can be regarded. The complete vehicle electrical system simulation can monitor currents and voltages on all components. Herby the influence of the fault case to other components of the electrical system can be visualized. Dimensioning of component parameters regarding safety aspects is possible hereby.

3) Contactor fault during battery charging

Open the mechanical contactors of the battery during charging process leads to transient effects in the HV-system since too much energy is delivered to the system. Figure 17 presents DC-link voltage and

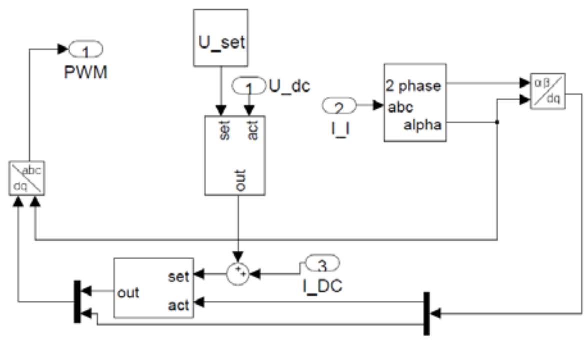

Fig. 13. Active rectifying control.

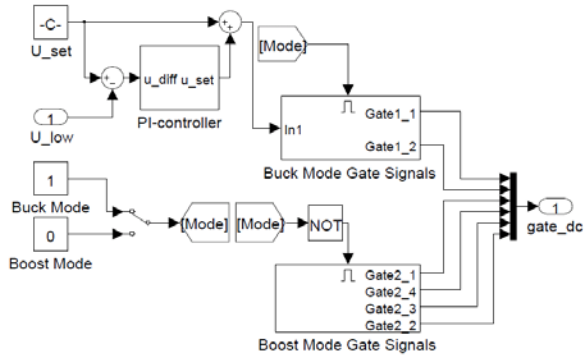

Fig. 14. Control of the bidirectional DC-DC converter.

charging current during fault operation. The current declines under strong oscillation to zero. The voltage oscillates and returns to the nominal value. The transient process is mainly influenced by parameters of the π-element cable model and the battery model itself. Here, both mechanical contactors open simultaneously. A single contactor fault can be considered and simulated, as well. The process of reconnection of the battery terminals during operation of the HV-system is another critical case, since transient reactions of voltage and currents are expected.

4) Influences of a HV-AC insulation fault to the HV-DC system

An insulation fault of one of the cables connecting the starter/generator with the power electronic circuit affects the HV-DC system. The error current can circulate via the car chassis, Y-capacitors and power electronics. Figure 18 depicts the error current measured directly behind the fault location. The shape of the current strongly depends on the cable parameters, the Y-capacitors and the actual switching condition of the power electronics. Regarding safety and efficiency of the HV-system these currents has to be monitored. By this simulation the cross coupling between the different voltage levels can be analyzed. Influences to vehicle components in the different system parts are in focus of research .

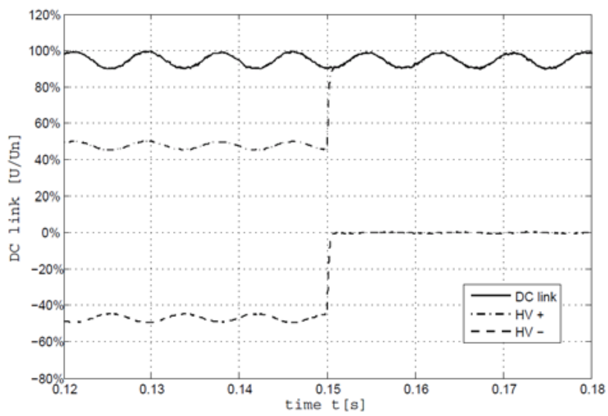

Fig. 15. Potentials of the DC-link during single insulation fault.

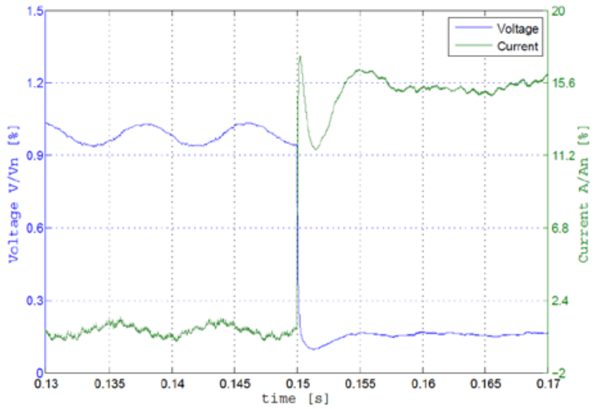

Fig. 16. Results of a short circuit fault to the DC-link.

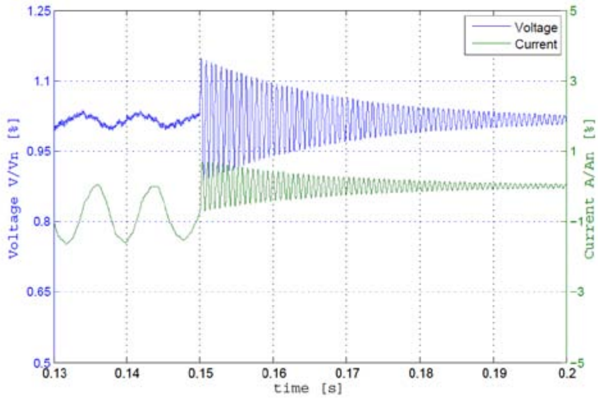

Fig. 17. Contactor fault during battery charging.

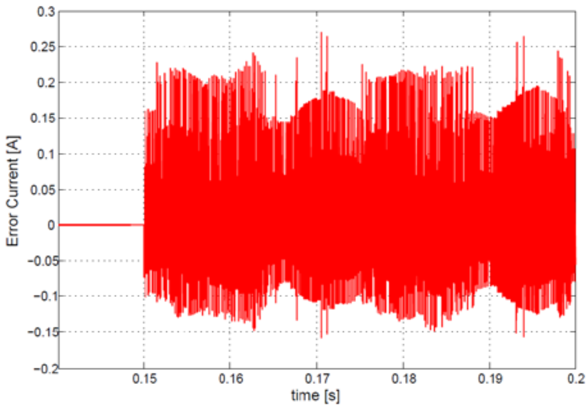

Fig. 18. Error current after HV-AC insulation fault.

III. Conclusions

This paper presents a combined method for the simulation of the dynamic behavior of electric voltages and currents in vehicle electrical systems during operation. The system topology is characterized. Component modeling by using electric equivalent circuits and transfer functions is discussed. The use of the circuit simulator PLECS is proposed to combine power electronic circuits with the simulation environment used. By this procedure, advantages of both software systems can be used. Various operating conditions and the implication on the vehicle electrical system can be simulated. The simulation results presented in this paper show deviations from the regular operation. Transient voltages, high short circuit currents or error currents resulting from insulation faults are simulated in this way. Other critical fault scenarios as load dumps can be analyzed as well. This fault situations are used for reliability and safety issues. The model can be parameterized for various vehicle electrical systems.

Another related research field is the simulation of lightning arcs. Due to the high voltages above the standard 12V system, lightning arcs occur after connection faults in the HV-system. Modeling techniques and the interaction with the simulation are under investigation and will be presented in following works.

References

[1] R. M. Fabis, *Beitrag zum Energiemanagement in Kfz-Bordnetzen*, Dissertation Technische Universität Berlin, 2006.

[2] D. W. Gao, C. Mi, A. Emadi, "Modeling and simulation of Electric and Hybrid Vehicles", *Proceedings of the IEEE,* vol 95, Issue 4, Pages: 729 – 745, April 2007.

[3] J. H. Allmeling, W. P. Hammer, "PLECS- Piece-wise Linear Electrical Circuit Simulation for Simulink", *Proceedings of the International Conference on Power Electronics and Drive Systems, 1999, PEDS '99,* vol 1, Pages: 355 – 360, July 1999.

[4] A. Tewari, *Modern Control Design with Matlab and Simulink,* John Wiley & Sons LTD., Chichester, 2002.

[5] N. Mohan, T.M. Undeland, W.P. Robbins, *Power Electronics,* John Wiley & Sons LTD., New Jersey, 2003.

[6] H.L. Chan, D. Sutanto, "A new battery model for use with battery energy storage systems and electric vehicle power systems", *Power Engineering Society Winter Meeting,* vol 1, Pages: 470 – 475, Jan. 2000.

[7] Y. Barsukov, "Cell-Type Specific Settings for Cell Imbalance Permanent Failure Thresholds", *Texas Instruments Application Report SLUA433,* 2007.

[8] S. Han and D. Divan, " Bi-Directional DC/DC Converters for Plug-in Hybrid Electric Vehicle (PHEV) Applications", *Applied Power Electronics Conference and Exposition, 2008, APEC 2008, Twenty-Third Annual IEEE, 24-28 Feb. 2008,* Pages: 784-789, Feb. 2008.

[9] O. García, L.A. Flores, J.A. Oliver, J.A Cobos, J. de la Peña, "Bi-Directional DC-DC Converters for Hybrid Vehicles", *Power Electronics Specialists Conference, 2005. PESC '05. IEEE 36th 16-16 June 2005,* Page(s):1881 - 1886, 2005 .

[10] S. Inoue, H. Akagi, "Voltage Control of a Bi-Directional Isolated DC/DC Converter for Medium-Voltage Motor Drives", *Power Conversion Conference - Nagoya, 2007. PCC '07 2-5 April 2007,* Page(s):1244 - 1250.

[11] H. de Paula, M.L.R. Chaves, D.A. Andrade, "A simple and accurate cable modeling suitable for high-frequency phenomena analysis in PWM motor drives", *Power Electronics Specialists Conference, PESC '05,* Pages: 680 – 686, 2005.

[12] J. R. Rodriguez, J. W. Dixon, J. R. Espinoza, J. Pontt, P. Lezana, "PWM Regenerative Rectifiers: State of the Art", *IEEE Transaction on Industrial Electronics,* Vol. 52, No.1, 2005.

[13] M. Malinowski, *Sensorless Control Strategies for Three-Phase Rectifiers,* Ph.D. thesis Warsaw University of Technology, 2001.